Natural Hazards
and Earth System
Sciences
Discussions

Reconstruction of flow conditions from 2004 Indian Ocean tsunami deposits at the Phra Thong island using a deep neural network inverse model

Rimali Mitra[1], Hajime Naruse[1], and Shigehiro Fujino[2]

[1]Division of Earth and Planetary Sciences, Graduate School of Science, Kyoto University, Kitashirakawa Oiwakecho, Kyoto, 606-8502, Japan.
[2]Faculty of Life and Environmental Sciences, University of Tsukuba, 1-1-1 Tennodai, Tsukuba, Ibaraki, 305-8572, Japan

Correspondence: Rimali Mitra (mitra.rimali.37z@st.kyoto-u.ac.jp)

Abstract. The 2004 Indian Ocean tsunami caused major topographic changes that resulted in significant economic losses and a large number of fatalities in the coastal areas. The estimation of tsunami flow conditions using inverse models has become a fundamental aspect of disaster mitigation and management. Here, in relation to the 2004 Indian Ocean tsunami, a case study involving the Phra Thong island in Thailand was conducted using inverse modeling that incorporates a deep neural network (DNN). The inverse analysis reconstructed the values of flow conditions such as maximum inundation length, flow velocity and maximum flow depth, sediment concentration from the post-tsunami survey around Phra Thong island. The quantification of uncertainty was also reported using the jackknife method. Using other models applied to areas in and around Phra Thong island, the predicted flow conditions were compared with the reported observed values and simulated results. The estimated depositional characteristics such as volume per unit area and grain-size distribution, were in line with the measured values from the field survey. These qualitative and quantitative comparisons demonstrated that the DNN inverse model is a potential tool for estimating the characteristics of modern tsunamis.

1 Introduction

On December 26, 2004, a Mw 9.1 earthquake triggered a devastating tsunami that affected the coastal areas and cities adjacent to the Indian Ocean, which resulted in extensive socio-economic damage and numerous fatalities in several countries including Thailand, Indonesia, Srilanka, India, Myanmar (Rossetto et al., 2007; Satake et al., 2006; Sinadinovski, 2006; Philibosian et al., 2017; Satake, 2014; Pari et al., 2008). In Thailand, 8300 people lost their lives, with 70 lives and a village of households were lost on the Phra Thong island in Phang-Nga province (Satake et al., 2006; Masaya et al., 2019). The total damage was estimated to amount to around USD 508 million, which equates to 2.2% of GDP which while the number of deaths was 4225, with the injured and missing cases and the cost reconstructing properties much lower than the overall damage value (Jayasuriya and McCawley, 2010; Suppasri et al., 2012).

An awareness of tsunami disaster prevention is the most essential criterion to reduce socioeconomic losses suffered by countries lying along the coastlines, such as Thailand, Japan, Indonesia, India and Srilanka etc (Lin et al., 2012). However, it

is well known that Japan's disaster mitigation system is better than those of the other aforementioned countries since disasters, such as earthquakes and tsunamis, occur more frequently in this nation (Doi, 2003). Indeed due to the lower tsunami risk and
25 the higher return period of high magnitude tsunamis (600 years), the degree of preparedness in terms of, for example, active sea-observation teams, effective evacuation techniques, and appropriate awareness remained in the early stage of development in Thailand (Suppasri et al., 2012). Suppasri et al. (2012) reported that, the nation has implemented post-tsunami precautionary measures such as, the construction of evacuation shelters at a safe height and distance from the coastline and of evacuation routes with evacuation regulations, memorial parks, appropriate structural design and land use management aimed at dealing
30 with tsunami waves. Meanwhile, a careful building of sea walls, and breakwaters has also been suggested for the area.

To propose appropriate regulations for evacuation plan and tsunami hazard mitigation, evaluating the extent to which tsunamis, travel inland in terms of flow velocity and the maximum height that the tsunamis could reach is important (Pignatelli et al., 2009). However, these flow parameters have not been directly measured, even for the 2004 Indian Ocean tsunami. It has been reported that the maximum elevation that a tsunami can reach (tsunami height) in Thailand, is between 5 and 15 m,
35 and Tsuji et al. (2006) reported a height of 19.6 m in Phra Thong island, while Rossetto et al. (2007) reported a peak tsunami height of 11 m and Satake (2005) and Jankaew et al. (2008) reported a tsunami height of 5 to 12 m in this area. such as flow velocity and depth, remain largely unknown. From an obtained video footage of the tsunami, Rossetto et al. (2007) reported a flow velocity of 6–8 m/s at the Khao Lak area and 3–4 m/s at Kamala beach. Other reported flow velocities from Thailand include 4 m/s at Phuket and 9 m/s at Khao Lak (Szczuciński et al., 2012; Mård Karlsson et al., 2009).

40 To obtain the onsite flow conditions essential to tsunami hazard mitigation in terms of devising future structural measures and levee construction, investigating tsunami deposits, which provide crucial information on the flow discharge and the extent of the tsunami inundation (Dawson and Shi, 2000; Udo et al., 2016; Sugawara and Goto, 2012; Furusato and Tanaka, 2014; Sugawara et al., 2014; Koiwa et al., 2018; Masaya et al., 2019), is important. It has been suggested that, after distinguishing tsunami deposits from other deposits such as flood or storm deposits through their sedimentological characteristics (Morton
45 et al., 2007; Switzer and Jones, 2008; Szczuciński et al., 2012), they can be used to reconstruct tsunami flow conditions (Jaffe and Gelfenbuam, 2007; Smith et al., 2007; Paris et al., 2009; Sugawara and Goto, 2012; Naruse and Abe, 2017; Tang et al., 2018). The preservation of sedimentary bedforms in the sand sheet, capping bedforms, sedimentary structure, texture, and facies models provides the evidence of flow direction and changes in flow energy and hydrodynamic aspects such as flow height and inundation length (Choowong et al., 2008; Switzer and Jones, 2008; Szczuciński et al., 2012). Other reconstructions
50 of the tsunami flow conditions at Khao Lak were completed using eyewitness reports, aerial videos, and photographs, while the extent of the damage was analyzed using field measurements and satellite imagery (Mård Karlsson et al., 2009). In addition, age data from the paleo-root horizon of mangroves, as well as an analysis of the sediment geochemistry and the diatom assemblages, also provided insights into the flow conditions of the 2004 Indian Ocean tsunami (Andrade et al., 2014; Sakuna et al., 2012; Sawai et al., 2009).

55 To reconstruct quantitative values of tsunami characteristics from the deposits, various numerical inverse models which incorporate sediment dynamics, and transport and depositional equations have been established (Jaffe et al., 2012; Johnson et al., 2016; Li et al., 2012; Sugawara and Goto, 2012; Yoshii et al., 2018). Recently, the deep neural network (DNN) inverse

model was proposed (Mitra et al., 2020) and was proven to be effective for reconstructing flow conditions via an examination

of the deposits of the 2011 Tohoku-oki tsunami. This model also provides some insight into the uncertainty quantification of

60 the estimated flow parameters using the jackknife method. The DNN inverse model predicted the tsunami flow conditions (e.g.,

maximum inundation length was 4045 m, flow velocity 5.4 m/s and maximum flow depth was 4.11 m) from Sendai plain with

the values very close to the observed values. Thus, this model has reasonable potential to estimate the hydraulic conditions

from the 2004 Indian Ocean tsunami that were not measured directly.

The Phra Thong island is one of the locations where the tsunami deposits were preserved without a great amount of topo-

65 graphic irregularities with almost no human interventions such as buildings, artificial structures in the island that caused very

less topographic disturbance in the tsunami deposits. The coastlines of Phra Thong island were severely eroded and retreated

by the 2004 tsunami and the presence of widespread mangrove forests with other waterborne plant debris helped in the identi-

fications of the extent and direction of the flow (Fujino et al., 2008, 2010). The island is a historically important location for the

study of tsunami deposits, with pre-2004 tsunami deposits preserved in inter-ridge swales and an overall extensive distribution

70 of paleotsunami deposits having been reported (Jankaew et al., 2008; Fujino et al., 2009). In fact, palaetsunami deposits have

been identified at Phra Thong isalnd, Thailand were identified by several research teams (Jankaew et al., 2008; Sawai et al.,

2009; Fujino et al., 2008, 2010; Brill et al., 2012b; Pham et al., 2017; Gouramanis et al., 2017; Masaya et al., 2019).

Here, we conduct an inverse analysis of the tsunami deposits measured at Phra Thong island, and reconsrtuct the tsunami

characteristics such as the maximum inundation length, flow velocity, maximum flow depth and sediment concentration. We

75 then use these flow conditions to estimate the spatial distribution of the volume per unit area and grain-size composition from

Phra Thong island and compare the distribution with the measured data. Our inverse analysis results could be used for designing

future tsunami hazard assessments and disaster mitigation strategies in Thailand.

2 Methodology

This study employed the DNN inverse model that was applied to the Sendai plain where the tsunami deposits of 2011 Tohoku-

80 oki tsunami was observed (Mitra et al., 2020). This model uses the forward model of FITTNUSS (the framework of inversion

of tsunami deposits considering transport of nonuniform unsteady suspension and sediment entrainment) (Naruse and Abe,

2017) to calculate the sediment transport and deposition from input parameters including the maximum run-up length, the

depth averaged flow velocity, the maximum flow depth, and sediment concentration at the seaward end. The forward model

can calculate the thickness and grain-size distribution along a 1D shoreline normal transect, which is used to train the DNN

85 inverse model. Here, we present a brief overview of the FITTNUSS forward model and the inverse model.

2.1 Forward model

The FITTNUSS forward model is based on the layer-averaged one-dimensional equations that take the following form:

$$\frac{\partial h}{\partial t} + \frac{\partial Uh}{\partial x} = 0, \tag{1}$$

$$\frac{\partial Uh}{\partial t} + \frac{\partial U^2 h}{\partial x} = ghS - \frac{1}{2}g\frac{\partial h^2}{\partial x} - u_*^2 \tag{2}$$

where h and U denote tsunami flow depth and the layer-averaged flow velocity respectively. The parameters t and x refer to the time and bed-attached streamwise coordinate set perpendicular to the shoreline and is positive landward; g is the gravitational acceleration; S is the bed slope, and $u*$ is the friction velocity. The sediment conservation equation was presented as follows:

$$\frac{\partial C_i h}{\partial t} + \frac{\partial U C_i h}{\partial x} = w_{si}(F_i E_{si} - r_{0i} C_i) \tag{3}$$

where C_i is considered as the volume concentration in the suspension of the ith grain-size class and w_{si}, E_{si}, r_{0i}, and F_i are the settling velocity, sediment entrainment coeffientcient, ratio of near-bed to layer-averaged concentration of the ith grain-size class and volumetric fraction of the sediment particles in the bed surface active layer, above the substrate respectively (Hirano, 1971).

For the sedimentation of tsunamis, the Exner equation of bed sediment continuity was used which is expressed as:

$$\frac{\partial \eta_i}{\partial t} = \frac{1}{1 - \lambda_p} w_{si}(r_{0i} C_i - F_i E_{si}) \tag{4}$$

where η_i refers to the volume per unit area (thickness) of the sediments of the ith grain-size class and λ_p accounts for the porosity of the bed sediment. As a result of the sedimentation, the grain-size distribution in the active layer varies with time (Hirano, 1971), and the rate of total sedimentation is expressed as follows:

Finally, using the assumptions proposed by (Soulsby et al., 2007) in which the velocity of tsunami run-up flow (U) was considered as uniform and steady but the flow depth varies with time, the flow dynamics of tsunamis were simplified in terms of the following equation:

$$\frac{\partial C_i}{\partial t} + U\frac{\partial C_i}{\partial x} = \frac{R_w}{H(Ut - x)}\left\{ w_{si}\left(F_i E_{si} - r_{0i} C_i\right)\right\}. \tag{5}$$

Here, R_w and H represent the maximum inundation length and flow depth of the tsunami at the seaward boundary of the transect, respectively. A transformed coordinate system and the implicit Euler's method has been applied to the equation to increase the computational efficiency (for more details, see Naruse and Abe (2017)).

Using the above equations, the forward model reproduces the spatial variation of the thickness and grain-size distribution of the tsunami deposit from the input values of the following (1) maximum distance of horizontal run-up (maximum inundation length), (2) maximum flow depth, (3) run-up velocity, and (4) sediment concentration of each grain-size class at the seaward boundary (Naruse and Abe, 2017). The grain-size classes selected for this inverse analysis were 659, 329, 164, 82 and 41 μm respectively.

2.2 Inverse Model

The DNN inverse model (Mitra et al., 2020) accepts grain-size and thickness distribution at an input layer of neural network (NN). The nodes in the input layers receive the values of the volume per unit area of all grain-size classes at the grid points of the forward model. Then, following the feed forward mechanism, the NN outputs the tsunami characteristics through the several hidden layers (Figure 1b) (Mitra et al., 2020).

Before applying the DNN inverse model to the natural tsunami deposits, it was trained using artificial training datasets of tsunami deposits produced by the repetition of the forward model calculation with randomly generated input values. Figure 1a shows the workflow for training and to applying the inverse model. First, the tsunami characteristics values were randomly produced, and the repetition of the forward model calculations using the generated tsunami characteristics produced artificial datasets of the thickness and grain-size distribution of the tsunami deposits to train the NN. The model prediction was evaluated according to the loss function defined as follows:

$$J = \frac{1}{N} \sum \left(I_k^{fm} - I_k^{NN} \right)^2 \qquad (6)$$

where I_k^{fm} is denoted as the teaching data that are the initial parameters used for producing in the training data and I_k^{NN} denotes the predicted parameters. This loss function quantifies how close the NN was to an ideal inverse model.

The weight coefficients in the NN were optimized to minimize the loss function in the training process (Wu et al., 2018; Mitra et al., 2020). Following the training process, the model could be applied to a natural dataset of tsunami deposits. The details of the hyperparameter selection and the step-by-step procedures of the model training are provided in Mitra et al. (2020).

To generate the training datasets, the present inverse model involves the ranges of input parameters that are the maximum inundation length, maximum flow velocity, maximum flow depth and sediment concentrations of five grain-size classes for generating the training datasets, which were 1700–4500 m, 2.0–10 m/s, 1.5–12 m and 0% to 2% respectively. The range of maximum inundation length can be modified depending on the field evidence of the extent of the tsunami deposit distribution. The range of parameters adopted in this study is applicable to most of the large-scale tsunami-inundated areas.

A sampling window to select the region for applying the inverse model from the entire distribution of the datasets had to be set, given that, in certain cases, the field measurements along the transect do not cover the entire distribution. In addition, the measurements at the distal part of the transect may contain large errors since the tsunami deposits in that area may be too thin for precise observations. The model had to be trained on a specific sampling window, and precision of the model prediction depending on the sampling window size was tested using the validation datasets. For more details on the significance and applicability of the sampling window, please refer to Mitra et al. (2020).

We have selected a sampling window size of 1700 m for our study which was chosen on the basis of the comparative results obtained from tests using different sampling window sizes as described in the results section. For this study area, the grid spacing in the fixed coordinates was 15 m, meaning the number of spatial grids used for the inversion was 113.

To apply the inverse model to the natural dataset, the interpolation of the measured data is had to be fitted into the fixed coordinate system of the forward model. Here, a 1D cubic interpolation was used on the natural dataset that provides values

Natural Hazards
and Earth System
Sciences

Open Access

Discussions

EGU
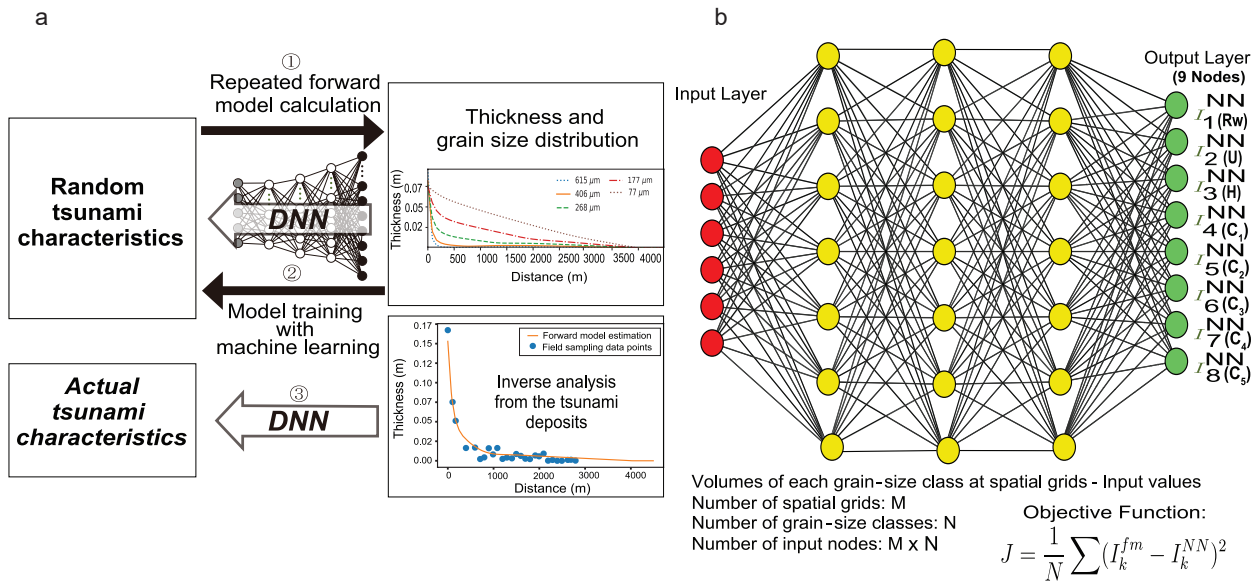
Figure 1. (a) Flow chart of the inverse model and (b) NN architecture of the DNN which predicts output maximum inundation length (R_w), flow velocity (U), maximum flow depth (H) and concentration of five grain-size classes (C_1 to C_5) (modified from Mitra et al. (2020))

at the positions between the data points of each sample. Since this procedure may have led to additional errors or bias in the results, checking the influence of the interpolation on the predictions of the inverse model using the subsampling of the artificial

150 datasets at the location of the outcrops was essential (Mitra et al., 2020).

The inverse model predicts the flow conditions, and the precision of the results was evaluated using the jackknife method. This method estimates the standard error of the statistics or a parameter of a population of interest from a random sample of data. The jackknife sample is described as the "leave-one-out" resample of the data. If there are N observations, there are N jackknife samples, each of which are $N-1$. If the sample of N observation is a set denoted as $x_1, x_2, ..., x_N$, the nth jackknife

155 sample is $x_1, ..., x_{n-1}, x_{n+1}, ..., x_N$. The pseudo-value estimation of the nth observation was then computed and an estimate of the standard error from the variance of the pseudo-values was obtained (Abdi and Williams, 2010; Mitra et al., 2020). For details of the jackknife method please refer to Mitra et al. (2020). The fluctuations of the jackknife standard errors varied depending on the sampling window sizes.
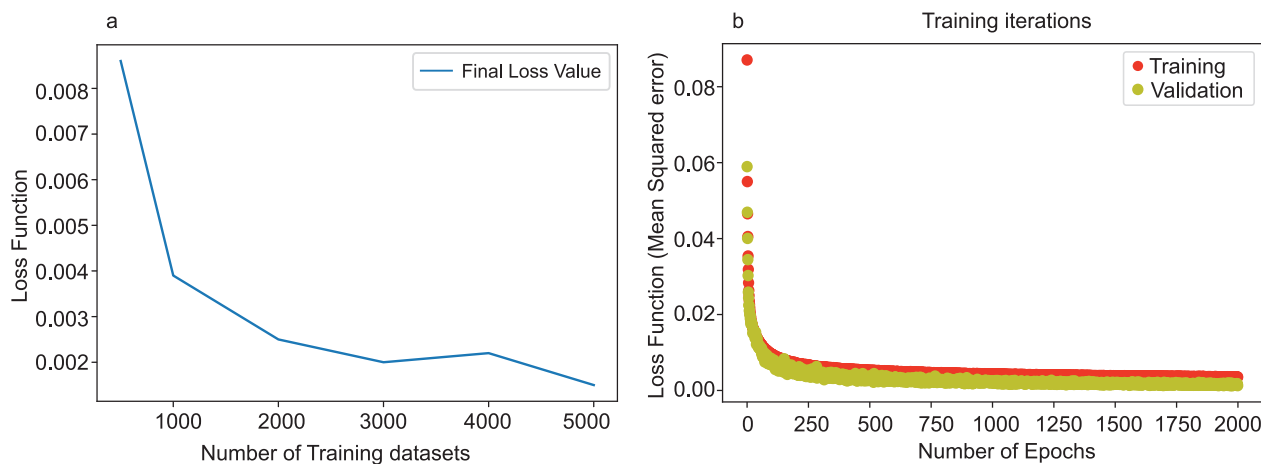
Figure 2. (a) Relationship between the loss function of the validation and the number of training datasets selected for the inverse model. The results of the training improved as the number of training datasets increased, while it slightly varied after 5000 training datasets. (b) History of learning indicated by the variation of the loss function (mean squared error). Both values of the loss function for the training and validation datasets reached a minimum value, indicating that overlearning did not occur.

3 Results

3.1 Training and testing of the inverse model

The DNN was trained using artificial datasets. The number of training datasets was chosen to be 5000 in this study. Figure 2a presents a plot graph of the relationship between the number of training datasets and the loss function of the validation dataset. The performance of the inverse model improved as the number of training datasets increased (Figure 2a), but there was only a slight improvement after the iteration of the forward model calculation exceeded 3000.

The training process proceeded with a certain number of epochs that indicated the repetition of the optimization calculation by the full dataset. Figure 2b shows that the present model was reasonably converged over 2000 epochs for both the training and validation performances. The loss function values of training and validation at the first epoch were 0.08 and 0.05, respectively. The final and lowest loss function at the final epoch was 0.0035 for the training datasets and 0.0013 for the validation datasets. The efficiency of the performance increased if the loss function reduced with the number of iterations or epochs over time.

After training the model, the predictions of the inverse model for the test datasets were plotted against the original values used for producing the datasets. Figure 3(a-h) shows that the eight predicted parameters from the artificial test datasets were

distributed along the 1:1 line in the graph indicating that the test results were correlated well with the original inputs. Figure 4(a-h) shows the histograms of the deviation of the estimated values predicted from the original values. Deviations were distributed in a relatively narrow range without large biases in relation to the true conditions, except in the case of the maximum flow depth which was slightly biased. The values of the predicted maximum flow depth were approximately 0.38 m lower than the input values.

3.2 Application of the DNN inverse model to the 2004 Indian Ocean tsunami

3.2.1 Study area

The study area is the Phra Thong island, an island situated off the west coast of Phang-Nga province (north of Phuket island) and the west coast of southern Thailand (Fig 6), and is adjacent to the Indian Ocean (Rodolfo, 1969). This study investigated the tsunami deposits distributed in the eastern coast of Phra Thong island, where the topography near the coastline is a flat plain that mainly consists of shore-parallel beach ridges with intervening swales (Brill et al., 2012a). The 2004 Indian Ocean tsunami flooded the area with waves higher than 6 m and an inundation limit of approximately 2 km inland (Tsuji et al., 2006; Fujino et al., 2010). The tsunami left a widespread sand sheet with a thickness of 5-20 cm (Jankaew et al., 2008; Fujino et al., 2010). Meanwhile, the presence of wet, peaty swales helped in the preservation of the tsunami deposits (Jankew et al., 2008, Fujino et al., 2009, Gouramanis et al. 2017). Given its natural topography with few artificial features, Phra Thong island is a rare case, that is useful for verifying tsunami sediment transport calculations with less uncertainty (Brill, 2012).

Figure 6 shows the location of Phra Thong island and the adjacent areas in Thailand where the tsunami deposits have been reported. We considered samples from 29 locations along the transect shown in Figure 6. The distance from pre-event the coastline to each sampling site was calculated by projecting of the sites to a flow parallel reference line (Fujino et al., 2010). Tsunami heights of 6.6, 7, and 12 m were reported near the transect where the coast was extensively eroded and had retreated several hundreds of meters. The shallow seafloors deposited large volumes of widely distributed sand sheet deposition along the coast, with the deposit is largely composed of medium to fine sand. The deposit became finer in a landward direction, becoming very fine at the landward limit of the tsunami.

The maximum inundation length was measured about 2000 m inland (Fujino et al., 2008, 2010) and the thickness of the tsunami deposits at a maximum of 12 cm, while this did oscillate a great deal for the first 1300 m from the shoreline. Meanwhile, the deposit exponentially thinned at the inland region. For more details on the thickness and grain-size distribution of the tsunami deposit, see the description of the transect of Phra Thong island provided by Fujino et al. (2010).

3.2.2 Inversion results

The inversion method was applied to the transect of Phra Thong island in view of reconstructing the flow conditions from the deposit of the 2004 Indian Ocean tsunami. The 1D cubic interpolation was applied to the dataset measured along the transect of Phra Thong island, before the inversion method was applied to the field dataset.
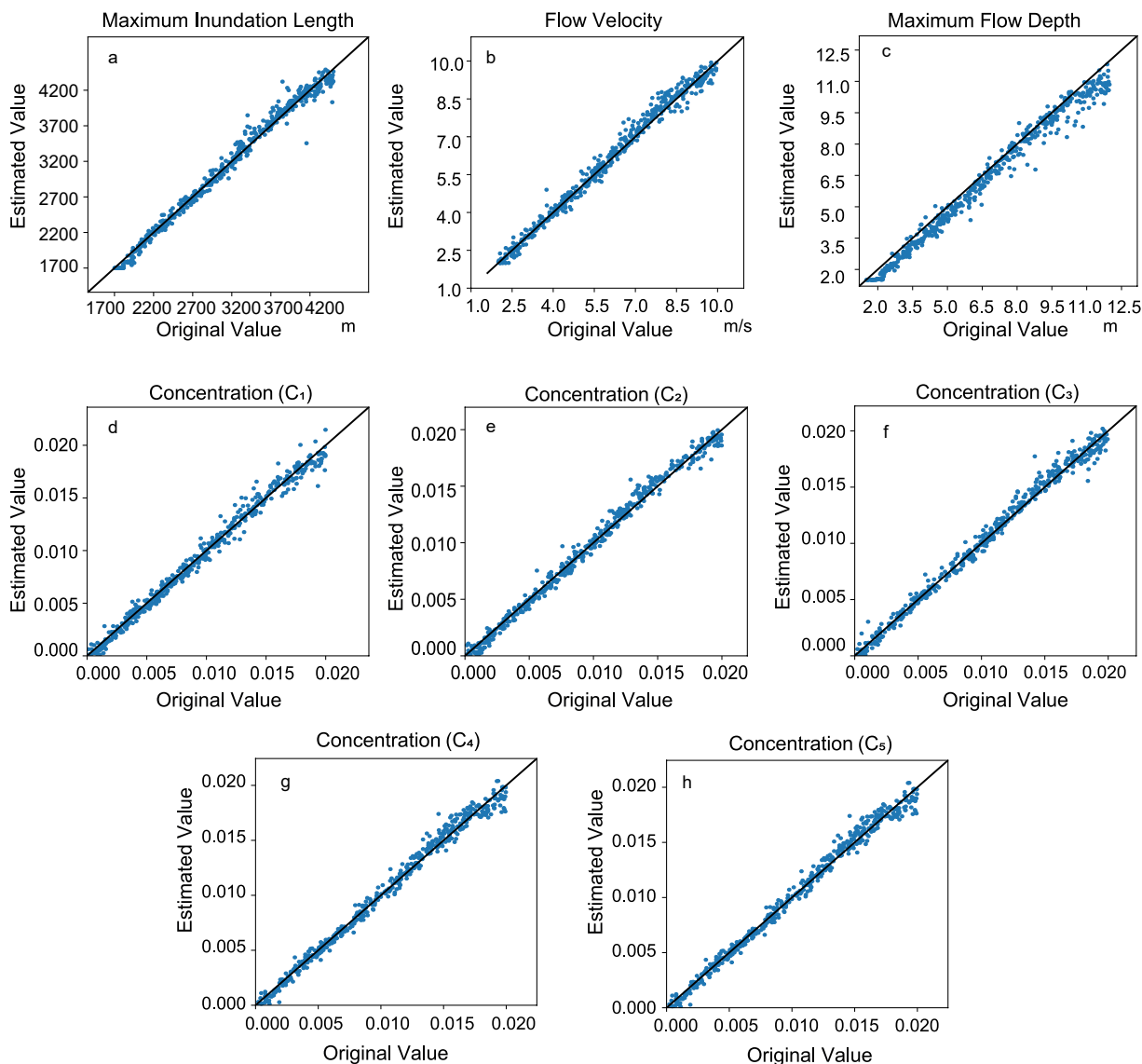
Figure 3. Performance verification of the model using artificial test datasets, indicating that the values estimated using the inverse model were plotted against the original values used for the production of the test datasets. Solid lines indicate a 1:1 relation and suggest good correlation.

We selected 1700 m as the length of the sampling window, which allowed for minimizing the uncertainty of the inverse analysis quantified via the jackknife method (Figure 7). The jackknife stand error was calculated in terms of different sampling
205   window sizes of the datasets (Figure 7), with the error decreasing as the sampling window was increased, with the exception of
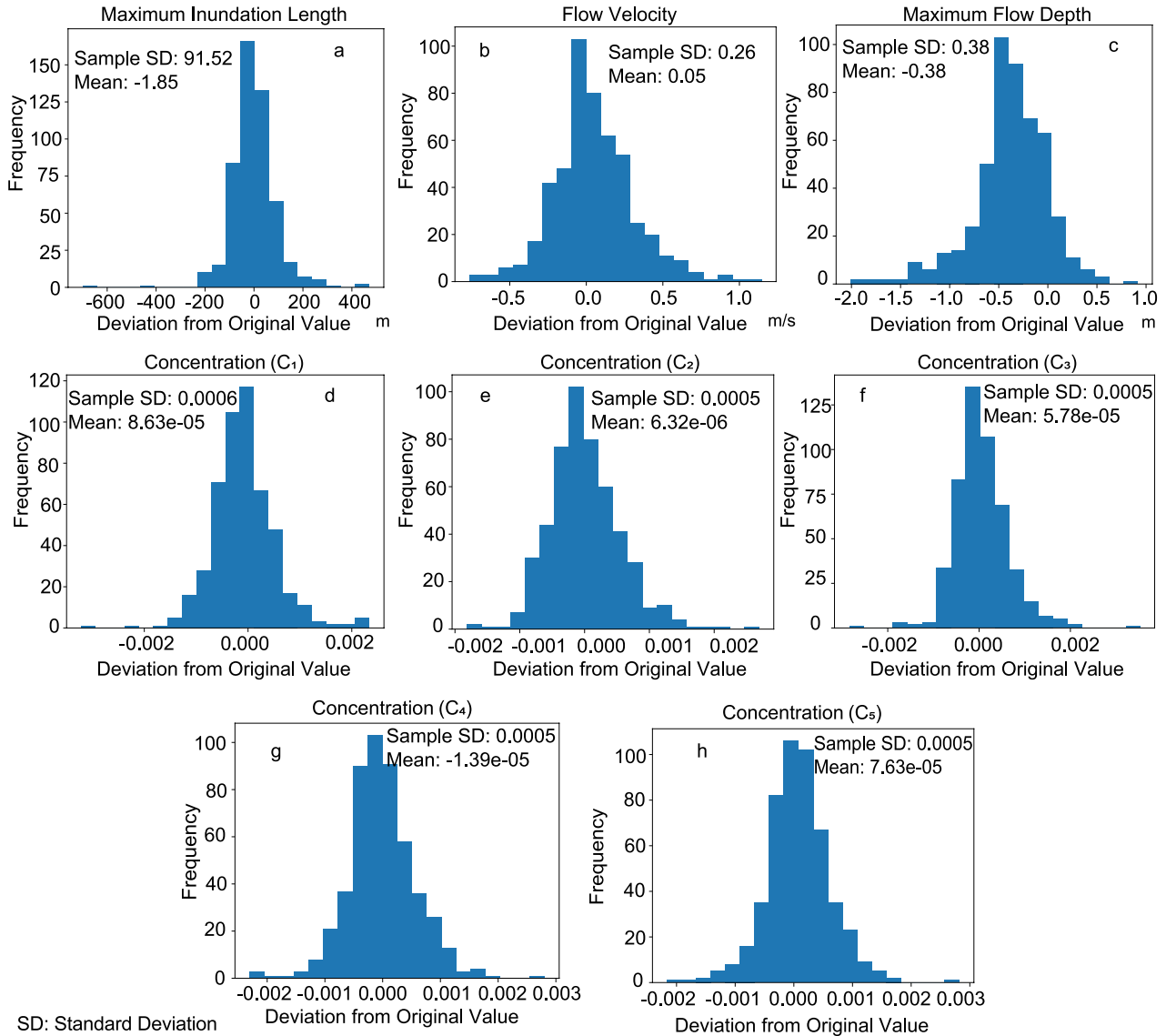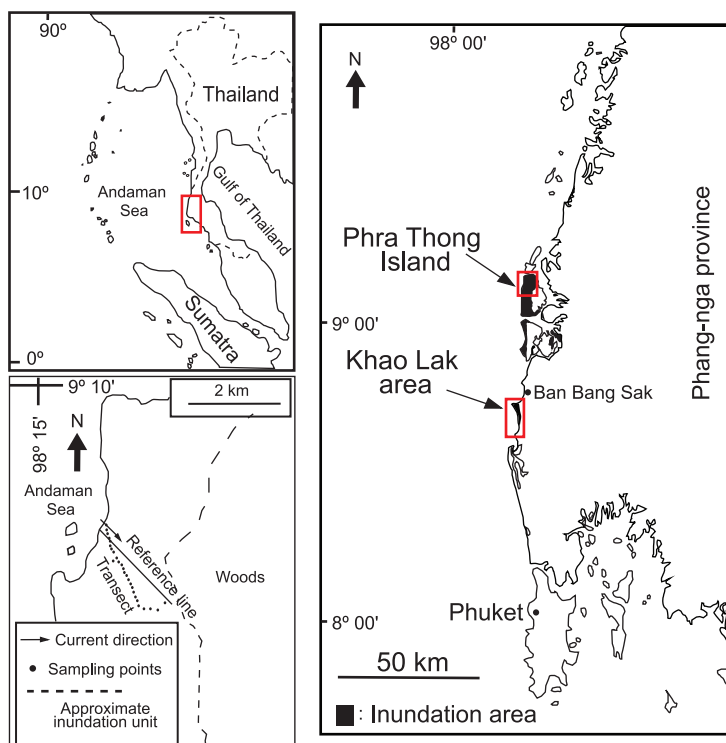
Figure 4. Histograms showing the deviation of the predicted results from the original values of the artificial test datasets.

the region above 1700 m. However, an increasing trend was observed for maximum flow depth, while the jackknife standard error became stable after 1500 m (Figure 7c). Thus, the 1700 m sampling window provided the best results in terms of the precision of the inversion. As described in the method section, the interpolation of the measured datasets at the computational grids may result in additional bias or errors from the inverse model. The subsampling analysis was thus conducted using artificial datasets.
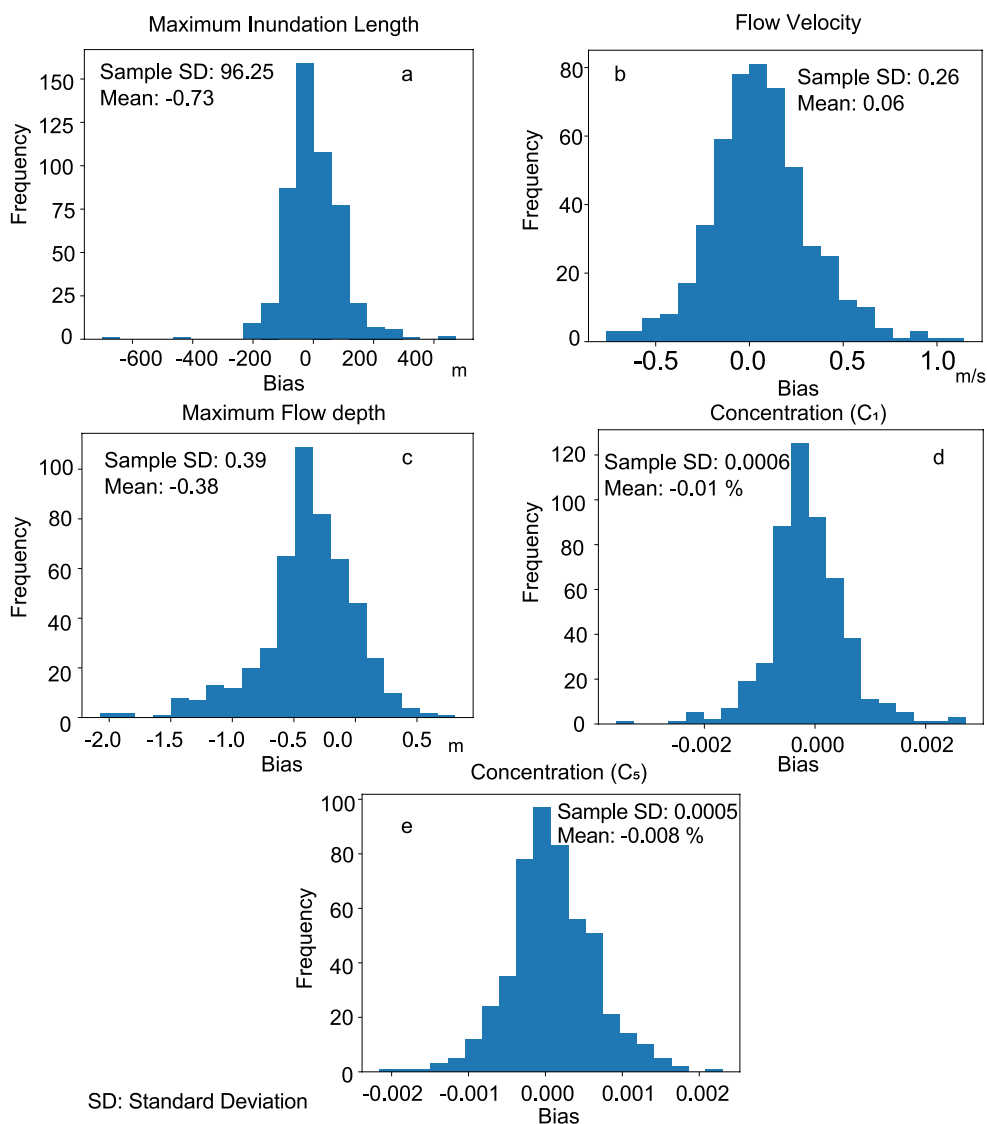
Figure 5. Histograms showing the variance and bias of predictions from the test datasets subsampled at the sampling locations of the transect in Phra Thong island.

The subsampling test demonstrated that the inversion model had a mean bias of -0.73 m for maximum inundation length (Figure 5). Meanwhile, the predicted results for the flow velocity was 4.46 m/s and it was 3.92 m for the maximum flow depth, with the mean bias obtained from the subsampling results being 0.06 m/s for flow velocity and -0.38 m for maximum flow depth, which were exactly in line with the values obtained from the testing of the trained DNN model without the subsampling test.

Figure 6. Histograms showing the variance and bias of the predictions from the test datasets subsampled at the sampling locations of the transect in Phra Thong island.

Table 1. Predicted results from the inverse model when applied to the 2004 Indian Ocean tsunami data obtained from Phra Thong island, Thailand. All reported standard error calculations were performed using a 95% confidence interval.

Parameters	Predicted Results	Mean Bias
Maximum Inundation Length	1700 m $\pm$ 17.73 m	-0.73 m
Flow Velocity	4.46 m/s $\pm$ 0.20 m/s	0.06 m/s
Maximum Flow Depth	3.92 m $\pm$ 0.17 m	-0.38 m
Concentration of C_1 (659 μm)	0.09% $\pm$ 0.016%	0.01%
Concentration of C_2 (329 μm)	0.27% $\pm$ 0.017%	7×10^{-4}%
Concentration of C_3 (164 μm)	0.25% $\pm$ 0.031%	0.005%
Concentration of C_4 (82 μm)	0.31% $\pm$ 0.009 %	1×10^{-4}%
Concentration of C_5 (41 μm)	0.07% $\pm$ 0.006%	0.008%

Table 1 shows the predicted flow conditions with a 95% confidence interval calculated by jacknife method (Figure 8). When using the jackknife standard error calculations, the maximum inundation length was 1700 m with 17.73 m range of
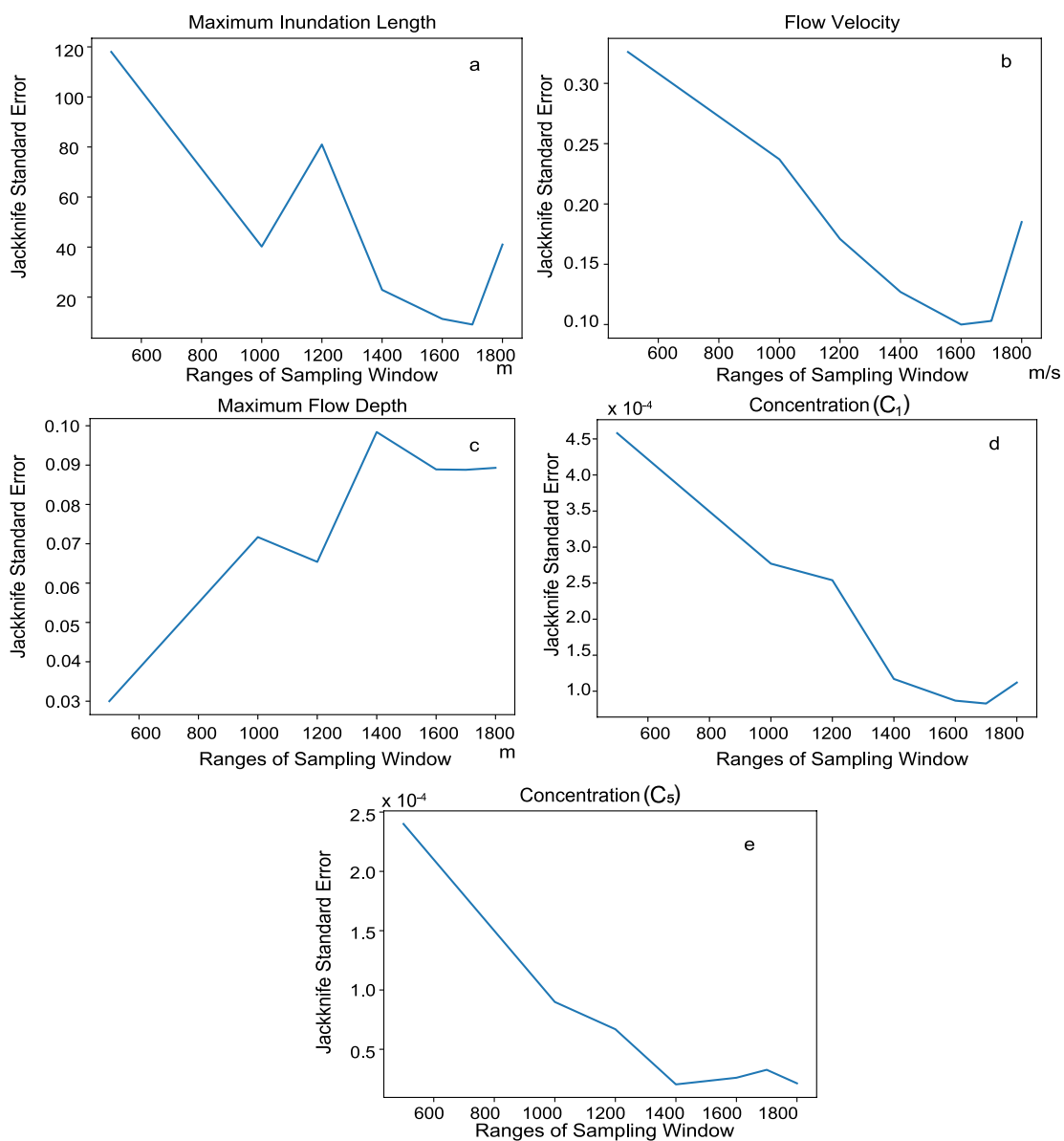
Natural Hazards
and Earth System
Sciences

Open Access

Discussions

EGU

Figure 7. Propagation of jackknife standard errors with different range of sampling window distances.

Natural Hazards
and Earth System
Sciences
Discussions
EGU
Open Access

uncertainty (Figure 8a), while the actual inundation length was approximately 2000 m (Fujino et al., 2010). Meanwhile, the estimated flow velocity was 4.46 m/s and the maximum flow depth was 3.92 m with jackknife standard error uncertainty values
220 0.20 m/s and 0.17 m, respectively (Figure 8b-c). The reconstructed total sediment concentration over five grain-size classes was approximately 1%, and the estimated values of each grain-size class ranged from 0.07%–0.31%. The jackknife error estimation shows the presence of errors were low such as 0.006%.

Finally, the forward model calculation was performed using the reconstructed flow conditions to estimate the spatial distribution of the volume per unit area and grain-size composition, and it was compared with the measured values from the transect
225 of Phra Thong island. Figure 9 shows the predicted spatial grain-size distribution was in line with the actual values from field measurements.

4   Discussion

4.1   The model's inversion performance

The training and testing of the DNN inverse model demostrated that this model has reasonable ability to predict tsunami
230 characteristics such as maximum inundation length, flow velocity, maximum flow depth and sediment concentrations. The final loss function values for the training and validation were 0.0035 and 0.0013 respectively which were close (0.0040 and 0.0018) to those reported by Mitra et al. (2020). The testing of the DNN inverse model was evaluated using artificial datasets of tsunami deposits. The scatter diagrams (Figure 3) of the predicted and true conditions indicate a good correlation, with no large deviation in the mode of the predicted values except for a slight bias in the maximum flow depth. While the model tended
235 to estimate the maximum flow depth values approximately 0.38 m higher on average, correcting the final results by adding the bias to the final reconstructed values from the original field data was possible. In Mitra et al. (2020), the reported bias for the maximum flow depth was approximately 0.5 m, while the sample standard deviation was around 0.40, which is close to the value in the present study (0.38 m).

Regarding the deviation of the predicted values from the true values, the sample standard deviation values were relatively
240 small for all parameters. The sample standard deviation for the maximum inundation length was as low as 91.52 m for a range of true values of 1700–4500 m, while that for flow velocity was 0.26 m/s for a range of true values of 2.0–10 m/s. Meanwhile, the average value for sediment concentration was around 0.05%. All these values were close to those reported by Mitra et al. (2020) (e.g., maximum inundation length, 77.03 m; flow velocity, 0.30 m/s, sediment concentration, 0.06%).

After the model was trained and tested, the test datasets were subsampled at the outcrop locations on Phra Thong island to
245 investigate the presence of bias in the predicted flow conditions due to the irregular distribution of the sampling points. The results implied that the irregularity of the outcrop distribution had little effect on the bias and errors of the inversion. In fact, the bias values for maximum inundation length, flow velocity, and sediment concentration were negligible (Figure 5a-e), while that for the maximum flow depth in the subsampling tests indicated no additional bias, implying that the sampling interval on Phra Thong was sufficient for the inverse analysis using the DNN model.
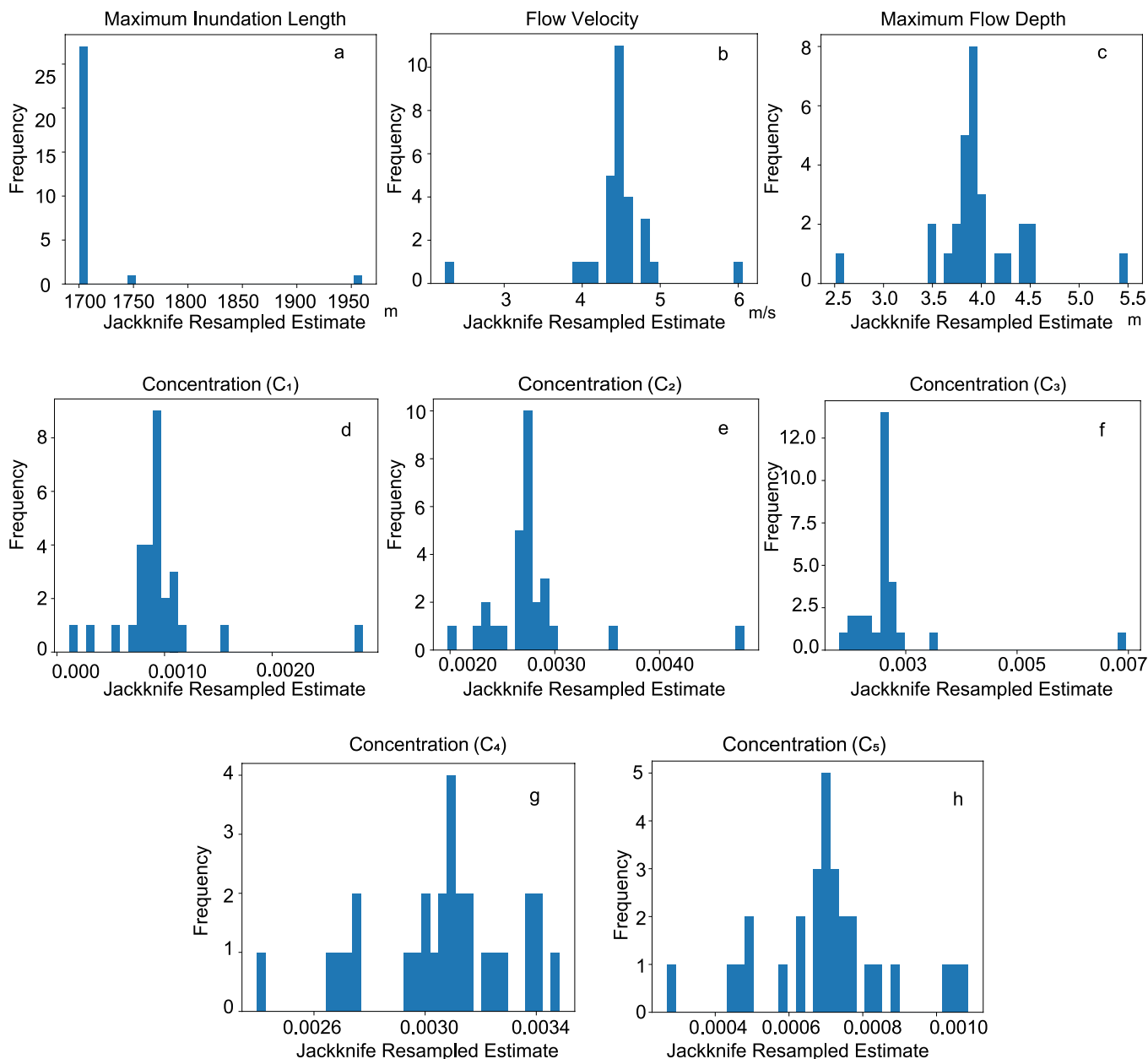
Figure 8. Jackknife estimates for the results predicted by the inverse model at the 1700 m sampling window, used to determine the uncertainty of the model.

To summarize, the performance of the trained DNN inverse model was identical to that of the model reported in Mitra et al. (2020) which successfully reconstructed various characteristics of 2011 the Tohoku-oki tsunami. It is noteworthy that Mitra
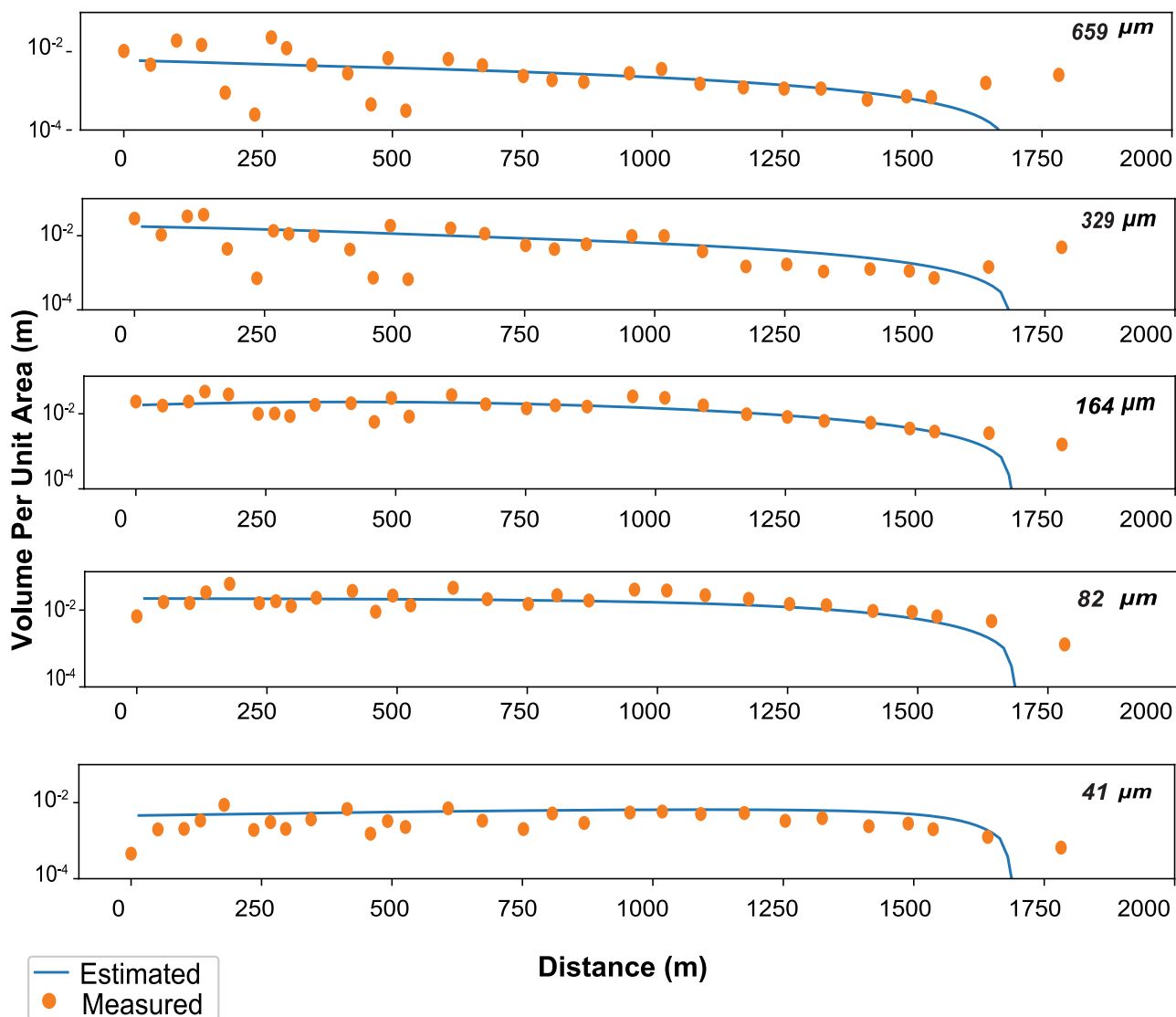
Figure 9. Spatial distribution of volume per unit area of five grain-size classes. Solid circles indicate the values measured by Fujino et al. (2010), and lines indicate the results of the forward model calculation obtained using parameters predicted by the DNN inverse model.

et al. (2020) used different numbers of grain-size class than used in our study, and they also employed different ranges of initial parameters for flow velocity and maximum inundation length. The modifications in the current study were necessary since the grain-size distribution of the tsunami deposits measured at Phra Thong island was considerably coarser than that measured

Natural Hazards
and Earth System
Sciences
Discussions

Open Access

EGU

255 in the Sendai plain. This change had close to zero effect on the performance of the inverse model, implying that the inverse method employed in this study is adaptable to various environments.

4.2   Verification of inversion results for the tsunami deposits

After the testing of the inverse model described above, we applied the model to the datasets obtained along the transect (Figure 6), and obtained the first quantitative estimates of the tsunami characteristics in Phra Thong island. While in situ measurements

260 of the 2004 Indian Ocean tsunami's activity on in Phra Thong island are not abundant, several surveys have reported the attendant inundation heights and run-up length of the tsunami in this region. Here we compare our inversion results with these in situ measurements of 2004 Indian Ocean tsunami.

The inversion results or the tsunami flow depth in this study were in the range of the in situ measurements. The DNN inverse model reconstructed the maximum inundation flow depth as 3.92±0.17 m at the sampling site, which was located 684 m from

265 the shoreline, when measured in the direction parallel to the flow direction (N154E). The data of tsunami inundation height, which present a summation of the flow depth and topographic height, were measured at Phra Thong island by several groups including the Tsuji and KSCOE groups (http://www.nda.ac.jp/ fujima/TMD/fujicom.html). The data points reported by the latter were 347 and 740 m from the shoreline, and were relatively close to the sampling site 1 (distances of 1.40 km and 1.37 km away from the sampling site 1). The observed values of the tsunami inundation heights at these sites were 7.1 and 6.7 m.

270 The KSCOE group also reported the inundation heights at four sites in Phra Thong island, which were 884–938 m from the shoreline, and relatively far from the transect (ca. 2.55 km from the sampling site 1), with the inundation heights found to be between 5.50-6.0 m at these sites. Meanwhile, the averaged elevation around the study area which was calculated from the topographic profiles provided by (Jankaew et al., 2008, 2011; Brill et al., 2012b), was approximately 2.90 m. The most seaward locations of the transect in Jankaew et al. (2011, 2008) were around 400 m from sampling site 1 in our study area. Hence, the

275 approximate estimate of the averaged observed maximum flow depth from Phra Thong area was 3.43 m, which was close to our predicted value. In fact, even after the bias correction of 0.38 m, the reconstructed value (4.3 m) was also within the range of the observed values. Hence, when based on the 1700 m sampling window size, the maximum flow depth reconstructed in this study was close to the reported measurements. However, certain amount of measurement and calculation error may have existed due to the local topographical variations. The model also estimated a maximum inundation length (1700 m) that was

280 close to the observed value apprximately 2000 m, which was measured at the inland end of the transect (Fujino et al., 2010).

4.3   Characteristics of the 2004 Indian Ocean tsunami on Phra Thong island

Our inversion results for the tsunami characteristics on Phra Thong island indicated that the tsunami inundation flow was typically uniform along the coastal area of Thailand. This study reconstructed the flow velocity of the tsunami as 4.46±0.20 m. Given that no direct observation values have been reported for this specific transect in Phra Thong island, this presented the first

285 estimate for this region. The reconstructed flow velocity in this region was close to the observed velocity in other regions of coastal areas in Thailand, albeit that a larger velocity was reported in the Khao Lak area. Rossetto et al. (2007) reported aerial video footage of the flow velocity, which was around 3-4 m/s on Phuket island (118 km south of our study area) and 6-8 m/s

Natural Hazards
and Earth System
Sciences
Discussions

Open Access

EGU

in the Khao lak area (43 km south of our study area). Elsewhere, Brill et al. (2014) used another inverse model (TsuSedMod) on the dataset from the Ban Bang Sak area, which is located around 35 km south of our study area and 20 km north of Khao Lak. Here, the predicted range values of flow velocity using TsuSedMod were 3.7–4.9 m/s. Given the values collected from the video footage (Rossetto et al., 2007) in relation to Phuket island, Khao lak area and the results reported by Brill et al. (2014), it is clear that most of the flow velocity values were around 4–5 m/s, apart from in the Khao Lak area. In fact, the flow depth measurement data from Khao Lak area also had exceptionally high values (Tsuji et al., 2006; Mård Karlsson et al., 2009), indicating that the tsunami inundation flow could have been locally enhanced by the topographic effects in this region. The flow velocity and depth of the 2004 Indian Ocean tsunami were similar in all other regions covering a 130 km area from Phuket to Phra Thong island.

4.4 Comparison with the results of existing 2D forward model

While the inverse analysis of tsunami deposits provides estimates of the flow characteristics in specific regions, two or three dimensional forward modeling is required to infer the spatial distribution of the flow parameters on a regional scale (Masaya et al., 2019; Li et al., 2012). The horizontal two dimensional forward model TUNAMI-N2 was applied to the Phra Thong island, to estimate the spatial distribution of the maximum flow depth in this area (Masaya et al., 2019). However, model appeared to have overestimated the maximum flow depth when compared with the measured values obtained by the KSCOE group (Choi et al., 2006),), with the former returning a flow depth of 6–8 m and the latter returning a depth of 4.2–3.8 m. This model is based on a fixed-source model where the initial water levels for a whole region are set along with the specific fault parameters. The model's results strongly depend on these fault parameters which should be iteratively modified to fit the measurement or distribution of the actual tsunami deposits. Moreover, the model of Masaya et al. (2019) employed single grain-size class for the reconstruction of the parameters from a larger area, which could have resulted in an erroneous estimation as the distribution of grain-size of tsunami deposits varies due to sediment transportation and deposition (Sugawara et al., 2014). In contrast, the DNN inverse model does not involve predefined conditions or thresholds to deduce the maximum flow depth. Here, the estimated flow characteristics and thickness distribution of the deposits by the DNN inverse model fitted well with the measured values, but they only apply to a local region. However, the DNN inverse model can potentially accept any type of forward models that can produce the distribution of tsunami deposits as training datasets. Thus, in future research, a two dimensional forward model such as the TUNAMI-N2 could be used as in junction with the for DNN inverse model to obtain the tsunami characteristics for a larger region.

5 Conclusions

The DNN inverse model demonstrated its efficiency in successfully reconstructing the hydraulic conditions of the 2004 Indian Ocean tsunami from the Phra Thong island, Thailand. The reconstructed maximum inundation length was 1700 m, while the flow velocity and maximum flow depth were 4.46 m/s and 3.92 m respectively. The uncertainty of the results also indicated

that simulated results did not contain a large range of values. Thus, this model can be applied to any areas consisting of low

320   land or flat areas to successfully reconstruct the tsunami flow conditions and can serve as a tool for tsunami hazard mitigation.

Code availability. The source codes and all other data of the DNN inverse model are available in Zenodo (https://doi.org/10.5281/zenodo.4075137)

Author contributions. H.N. designed the research; H.N. and R.M. performed the research; S.F. contributed the data from the Thailand area and analyzed the grain-size distribution; R.M. and H.N. wrote the paper.

325   *Competing interests.* The authors declare no competing interests.

Natural Hazards
and Earth System
Sciences

Open Access

EGU

Discussions

References

330 Abdi, H. and Williams, L. J.: Jackknife, Encyclopedia of research design, 2, 2010.

Andrade, V., Rajendran, K., and Rajendran, C.: Sheltered coastal environments as archives of paleo-tsunami deposits: Observations from the 2004 Indian Ocean tsunami, J Asian Earth Sci, 95, 331–341, 2014.

Brill, D.: The Tsunami History of Southwest Thailand: Recurrence, Magnitude and Impact of Palaeo-tsunamis Inferred from Onshore Deposits, Ph.D. thesis, Universitäts-und Stadtbibliothek Köln, 2012.

335 Brill, D., Klasen, N., Brückner, H., Jankaew, K., Scheffers, A., Kelletat, D., and Scheffers, S.: OSL dating of tsunami deposits from Phra Thong Island, Thailand, Quat Geochronol, 10, 224–229, 2012a.

Brill, D., Klasen, N., Jankaew, K., Brückner, H., Kelletat, D., Scheffers, A., and Scheffers, S.: Local inundation distances and regional tsunami recurrence in the Indian Ocean inferred from luminescence dating of sandy deposits in Thailand, Nat. Hazards Earth Syst. Sci., 12, 2177–2192, 2012b.

340 Brill, D., Pint, A., Jankaew, K., Frenzel, P., Schwarzer, K., Vött, A., and Brückner, H.: Sediment transport and hydrodynamic parameters of tsunami waves recorded in onshore geoarchives, J. Coastal Res., 30, 922–941, 2014.

Choi, B. H., Hong, S. J., and Pelinovsky, E.: Distribution of runup heights of the December 26, 2004 tsunami in the Indian Ocean, Geophys. Res. Lett., 33, 2006.

Choowong, M., Murakoshi, N., Hisada, K., Charoentitirat, T., Charusiri, P., Phantuwongraj, S., Wongkok, P., Choowong, A., Subsayjun, R.,
345 Chutakositkanon, V., , Jankaew, K., and Kanjanapayont, P.: Flow conditions of the 2004 Indian Ocean tsunami in Thailand, inferred from capping bedforms and sedimentary structures, Terra Nova, 20, 141–149, 2008.

Dawson, A. G. and Shi, S.: Tsunami deposits, Pure Appl. Geophys., 157, 875–897, 2000.

Doi, K.: Tsunami warning system in Japan, in: Early Warning Systems for Natural Disaster Reduction, edited by Zschau, J. and Küppers, A., pp. 537–541, Springer, 2003.

350 Fujino, S., Naruse, H., Suphawajruksakul, A., Jarupongsakul, T., Murayama, M., and Ichihara, T.: Thickness and grain-size distribution of Indian Ocean tsunami deposits at Khao Lak and Phra Thong Island, south-western Thailand, in: Tsunamiites, edited by Shiki, T., Tsuji, Y., T, Y., and K, M., pp. 123–132, Elsevier, 2008.

Fujino, S., Naruse, H., Matsumoto, D., Jarupongsakul, T., Sphawajruksakul, A., and Sakakura, N.: Stratigraphic evidence for pre-2004 tsunamis in southwestern Thailand, Mar. Geol., 262, 25–28, 2009.

355 Fujino, S., Naruse, H., Matsumoto, D., Sakakura, N., Suphawajruksakul, A., and Jarupongsakul, T.: Detailed measurements of thickness and grain size of a widespread onshore tsunami deposit in Phang-nga Province, southwestern Thailand, Isl. Arc, 19, 389–398, 2010.

Furusato, E. and Tanaka, N.: Maximum sand sedimentation distance after backwash current of tsunami—Simple inverse model and laboratory experiments, Mar. Geol., 353, 128–139, 2014.

Gouramanis, C., Switzer, A. D., Jankaew, K., Bristow, C. S., Pham, D. T., and Ildefonso, S. R.: High-frequency coastal overwash deposits
360 from Phra Thong Island, Thailand, Sci. Rep., 7, 43 742, 2017.

Hirano, M.: River bed degradation with armoring, Proceedings of Japan Society of Civil Enginees, 1971, 55–65, 1971.

Jaffe, B. E. and Gelfenbuam, G.: A simple model for calculating tsunami flow speed from tsunami deposits, Sediment. Geol., 200, 347–361, 2007.

Jaffe, B. E., Goto, K., Sugawara, D., Richmond, B. M., Fujino, S., and Nishimura, Y.: Flow speed estimated by inverse modeling of sandy
365   tsunami deposits: results from the 11 March 2011 tsunami on the coastal plain near the Sendai Airport, Honshu, Japan, Sediment. Geol.,
      282, 90 – 109, 2012.

Jankaew, K., Atwater, B. F., Sawai, Y., Choowong, M., Charoentitirat, T., Martin, M. E., and Prendergast, A.: Medieval forewarning of the
      2004 Indian Ocean tsunami in Thailand, Nature, 455, 1228–1231, 2008.

Jankaew, K., Martin, M. E., Sawai, Y., and Prendergast, A. L.: Sand sheets on a beach-ridge plain in Thailand: identification and dating of
370   tsunami deposits in a far-field tropical setting, The Tsunami Threat–Research and Technology, edited by: Mörner, NA, pp. 299–324, 2011.

Jayasuriya, S. K. and McCawley, P.: The Asian tsunami: aid and reconstruction after a disaster, Edward Elgar Publishing, 2010.

Johnson, J. P., Delbecq, K., Kim, W., and Mohrig, D.: Experimental tsunami deposits: Linking hydrodynamics to sediment entrainment,
      advection lengths and downstream fining, Geomorphology, 253, 478–490, 2016.

Koiwa, N., Takahashi, M., Sugisawa, S., Ito, A., Matsumoto, H., Tanavud, C., and Goto, K.: Barrier spit recovery following the 2004 Indian
375   Ocean tsunami at Pakarang Cape, southwest Thailand, Geomorphology, 306, 314–324, 2018.

Li, L., Qiu, Q., and Huang, Z.: Numerical modeling of the morphological change in Lhok Nga, west Banda Aceh, during the 2004 Indian
      Ocean tsunami: understanding tsunami deposits using a forward modeling method, Nat. Hazards, 64, 1549–1574, 2012.

Lin, A., Ikuta, R., and Rao, G.: Tsunami run-up associated with co-seismic thrust slip produced by the 2011 Mw 9.0 Off Pacific Coast of
      Tohoku earthquake, Japan, Earth Planet. Sci. Lett., 337, 121–132, 2012.

380 Mård Karlsson, J., Skelton, A., Sanden, M., Ioualalen, M., Kaewbanjak, N., Pophet, N., Asavanant, J., and von Matern, A.: Reconstructions
      of the coastal impact of the 2004 Indian Ocean tsunami in the Khao Lak area, Thailand, J. Geophys. Res.: Oceans, 114, 2009.

Masaya, R., Suppasri, A., Yamashita, K., Imamura, F., Gouramanis, C., and Leelawat, N.: Investigating beach erosion related with its recovery
      at Phra Thong Island, Thailand caused by the 2004 Indian Ocean tsunami, Nat. Hazards Earth Syst. Sci. Discuss., pp. 1–22, 2019.

Mitra, R., Naruse, H., and Abe, T.: Estimation of Tsunami Characteristics from Deposits: Inverse Modeling using a Deep-Learning Neural
385   Network, J. Geophys. Res.: Earth Surf., 125, e2020JF005 583, https://doi.org/10.1029/2020JF005583, https://agupubs.onlinelibrary.wiley.
      com/doi/abs/10.1029/2020JF005583, 2020.

Morton, R. A., Gelfenbaum, G., and Jaffe, B. E.: Physical criteria for distinguishing sandy tsunami and storm deposits using modern exam-
      ples, Sediment. Geol., 200, 184–207, 2007.

Naruse, H. and Abe, T.: Inverse Tsunami Flow Modeling Including Nonequilibrium Sediment Transport, With Application to Deposits From
390   the 2011 Tohoku-Oki Tsunami, J. Geophys. Res.: Earth Surf., 122, 2159–2182, 2017.

Pari, Y., Murthy, M. R., Kumar, J. S., Subramanian, B., and Ramachandran, S.: Morphological changes at Vellar estuary, India—Impact of
      the December 2004 tsunami, J. Environ. Manage., 89, 45–57, 2008.

Paris, R., Wassmer, P., Sartohadi, J., Lavigne, F., Barthomeuf, B., Desgages, E., Grancher, D., Baumert, P., Vautier, F., Brunstein, D., and G,
      C.: Tsunamis as geomorphic crises: lessons from the December 26, 2004 tsunami in Lhok Nga, west Banda Aceh (Sumatra, Indonesia),
395   Geomorphology, 104, 59–72, 2009.

Pham, D. T., Gouramanis, C., Switzer, A. D., Rubin, C. M., Jones, B. G., Jankaew, K., and Carr, P. F.: Elemental and mineralogical analysis
      of marine and coastal sediments from Phra Thong Island, Thailand: Insights into the provenance of coastal hazard deposits, Mar. Geol.,
      385, 274–292, 2017.

Philibosian, B., Sieh, K., Avouac, J.-P., Natawidjaja, D. H., Chiang, H.-W., Wu, C.-C., Shen, C.-C., Daryono, M. R., Perfettini, H., Suwargadi,
400   B. W., et al.: Earthquake supercycles on the Mentawai segment of the Sunda megathrust in the seventeenth century and earlier, J. Geophys.
      Res.: Solid Earth, 122, 642–676, 2017.

Natural Hazards
and Earth System
Sciences

Discussions

Pignatelli, C., Sansò, P., and Mastronuzzi, G.: Evaluation of tsunami flooding using geomorphologic evidence, Mar. Geol., 260, 6–18, 2009.

Rossetto, T., Peiris, N., Pomonis, A., Wilkinson, S., Del Re, D., Koo, R., and Gallocher, S.: The Indian Ocean tsunami of December 26, 2004: observations in Sri Lanka and Thailand, Nat. Hazards, 42, 105–124, 2007.

405 Sakuna, D., Szczuciński, W., Feldens, P., Schwarzer, K., and Khokiattiwong, S.: Sedimentary deposits left by the 2004 Indian Ocean tsunami on the inner continental shelf offshore of Khao Lak, Andaman Sea (Thailand), Earth, planets and space, 64, 11, 2012.

Satake, K.: The December 26, 2004 Sumatra Earthquake Tsunami, Tsunami Field Survey around Phuket, Thailand, http://www.drs.dpri.kyoto-u.ac.jp/sumatra/thailand/phuket_survey_e.html, 2005.

Satake, K.: Advances in earthquake and tsunami sciences and disaster risk reduction since the 2004 Indian ocean tsunami, Geoscience Letters, 410 1, 15, 2014.

Satake, K., Aung, T. T., Sawai, Y., Okamura, Y., Win, K. S., Swe, W., Swe, C., Swe, T. L., Tun, S. T., Soe, M. M., O, T. Z., and Z, S. H.: Tsunami heights and damage along the Myanmar coast from the December 2004 Sumatra-Andaman earthquake, Earth, planets and space, 58, 243–252, 2006.

Sawai, Y., Jankaew, K., Martin, M. E., Prendergast, A., Choowong, M., and Charoentitirat, T.: Diatom assemblages in tsunami deposits 415 associated with the 2004 Indian Ocean tsunami at Phra Thong Island, Thailand, Mar. Micropaleontol, 73, 70–79, 2009.

Sinadinovski, C.: The event of 26th of December 2004–the biggest earthquake in the world in the last 40 years, Bulletin of Earthquake Engineering, 4, 131–139, 2006.

Smith, D., Foster, I. D., Long, D., and Shi, S.: Reconstructing the pattern and depth of flow onshore in a palaeotsunami from associated deposits, Sediment. Geol., 200, 362–371, 2007.

420 Soulsby, R., Smith, D., and Ruffman, A.: Reconstructing tsunami run-up from sedimentary characteristics - a simple mathematical model, Coastal Sediments, 7, 1075–1088, 2007.

Sugawara, D. and Goto, K.: Numerical modeling of the 2011 Tohoku-oki tsunami in the offshore and onshore of Sendai Plain, Japan, Sediment. Geol., 282, 110–123, 2012.

Sugawara, D., Goto, K., and Jaffe, B. E.: Numerical models of tsunami sediment transport—Current understanding and future directions, 425 Mar. Geol., 352, 295–320, 2014.

Suppasri, A., Muhari, A., Ranasinghe, P., Mas, E., Shuto, N., Imamura, F., and Koshimura, S.: Damage and reconstruction after the 2004 Indian Ocean tsunami and the 2011 Great East Japan tsunami, Journal of Natural Disaster Science, 34, 19–39, 2012.

Switzer, A. D. and Jones, B. G.: Large-scale washover sedimentation in a freshwater lagoon from the southeast Australian coast: sea-level change, tsunami or exceptionally large storm?, The Holocene, 18, 787–803, 2008.

430 Szczuciński, W., Rachlewicz, G., Chaimanee, N., Saisuttichai, D., Tepsuwan, T., and Lorenc, S.: 26 December 2004 tsunami deposits left in areas of various tsunami run up in coastal zone of Thailand, Earth, planets and space, 64, 5, 2012.

Tang, H., Wang, J., Weiss, R., and Xiao, H.: TSUFLIND-EnKF: Inversion of tsunami flow depth and flow speed from deposits with quantified uncertainties, Mar. Geol., 396, 16–25, 2018.

Tsuji, Y., Namegaya, Y., Matsumoto, H., Iwasaki, S.-I., Kanbua, W., S, M., and Meesuk, V.: The 2004 Indian tsunami in Thailand: Surveyed 435 runup heights and tide gauge records, Earth, planets and space, 58, 223–232, 2006.

Udo, K., Takeda, Y., and Tanaka, H.: Coastal morphology change before and after 2011 off the Pacific coast of Tohoku earthquake tsunami at Rikuzen-Takata coast, Coastal Engineering Journal, 58, 1640 016–1, 2016.

Wu, L., Tian, F., Xia, Y., Fan, Y., Qin, T., Jian-Huang, L., and Liu, T.-Y.: Learning to teach with dynamic loss functions, in: Advances in Neural Information Processing Systems, pp. 6466–6477, 2018.

440   Yoshii, T., Tanaka, S., and Matsuyama, M.: Tsunami inundation, sediment transport, and deposition process of tsunami deposits on coastal lowland inferred from the Tsunami Sand Transport Laboratory Experiment (TSTLE), Mar. Geol., 400, 107–118, 2018.